Int. J. Appl. Math. Comput. Sci., 2025, Vol. 35, No. 4, 703–717
DOI: 10.61822/amcs-2025-0050

DATA DRIVEN INVENTORY CONSENSUS CONTROL FOR A SUPPLY CHAIN SYSTEM WITH A DESIGN CHANGE

LINGLING FAN [a], XIANGCHEN ZENG [a,*], SHUANGSHUANG XIONG [a], QINGKUI LI [a]

[a] School of Automation
Beijing Information Science and Technology University
No. 12, Xiaoying East Road, Haidian District, Beijing, China
e-mail: {2023020407,linglingfan}@bistu.edu.cn

The production and supply chain system is a complex nonlinear network comprising suppliers, manufacturers, distributors, retailers, and other entities. The collaborative evolution process for such a system is vitally important, especially when the system undergoes design changes. In this paper, the data-driven inventory consensus problem for production and supply chain systems is studied while considering design changes. Firstly, the production and supply chain system is modeled as a multi-agent one and the collaborative process of the production and supply chain is formulated as the system topology structure switching. Secondly, a digraph data-driven consensus control protocol is proposed to achieve inventory level consensus tracking with respect to a predefined reference trajectory in production and supply chain systems. Thirdly, when a design change occurs, the saturation function is introduced for the protocol design, which helps address the productivity limitation problem. Lastly, with the help of the contracting mapping principle, the convergence analysis is carried out, demonstrating the effectiveness of the proposed data-driven consensus approach through a numerical simulation example.

Keywords: consensus, data-driven, multi-agent, supply chain.

1. Introduction

Product design and manufacturing are closely related to the corresponding supply chains (Patalas-Maliszewska *et al.*, 2024). The collaborative evolution process for the production and supply chains constitutes a complex nonlinear network system composed of suppliers, manufacturers, distributors, retailers, and other entities (Xu *et al.*, 2021; Clempner and Poznyak, 2023). The product manufacturing process is typically considered a critical component of a supply chain, and the dynamic properties of the supply chain system can be reflected in the rate of change of production inventory levels (Patalas-Maliszewska *et al.*, 2022). It is well recognized that pursuing synchronous evolution is the most important task in an intelligent manufacturing system (Li *et al.*, 2023). Therefore, effective management and control of the supply chain system can reduce operational costs, improve customer satisfaction, and yield significant economic benefits. Recent advances in information technology have generated significant interest and notable achievements in supply chain system research (Sarimveis *et al.*, 2008; Chan and Zhang, 2011; Snyder and Shen, 2019; Li *et al.*, 2020; Darmawan *et al.*, 2021; Coopmans *et al.*, 2021). The current control system research predominantly relies on mathematical models derived from various physical mechanisms (Rodrigues and Boukas, 2006; Ignaciuk, 2015). The focus is mainly on static or simple linear system models. With the rapid development of information technology, dramatic changes have occurred in production and supply chain systems. Simple models cannot adequately capture the complex dynamics and evolving communication topology among system nodes. As the scale of the enterprise grows larger, manufacturing techniques, production equipment, and production processes become more complicated. It has become increasingly difficult to control, forecast, and evaluate the dynamic processes of supply chain systems. The vast operational and evolutionary data generated by these systems exacerbates this challenge. A question naturally arises: How can the vast amount of offline data and knowledge be effectively utilized when it is challenging to establish a more accurate

*Corresponding author

mechanistic model of the product and supply chain system? Data-driven techniques, which utilize only input-output data without requiring mathematical models, provide powerful alternatives for system analysis and synthesis. This is the primary motivation for current.

When we refer to data-driven control, we typically mean that the control approach is not reliant on any explicit or implicit information about the mathematical model of the system. Typical data-driven control approaches, according to the literature (Hou and Wang, 2013; Xiong and Hou, 2021), can be categorized as model-free adaptive control (MFAC) (Hou, 1994; Hou and Jin, 2013), iterative learning control (Ahn *et al*., 2007; Chi *et al*., 2012) and neural network control (Gomi and Kawato, 1993; Ge *et al*., 2013). Among these data-driven control approaches, MFAC has been developed within a systematic framework, making it an effective tool for handling discrete-time nonlinear systems with unknown dynamics (Haou and Jin, 2013; 2010). The merit of this approach originates from the proposed dynamical linearization technique, which introduces the so-called pseudo partial derivative for the nonlinear system. This technique does not require identification of unmodeled dynamics; only input-output data is needed. Therefore, it is suitable for complex systems that are difficult to model precisely, especially for product and supply chain systems that involve numerous unknown nonlinear models. MFAC thus offers an effective solution for a data-driven inventory consensus in production and supply chain systems undergoing design changes. This is another motivation for this paper.

On the other hand, the production and supply chain system, due to its distributed nature, is a complex network (Clempner and Poznyak, 2023). Here each node is expected to include a subchain for the convenience of expressing the mathematical model. This subchain comprises various entities such as suppliers, manufacturers, distributors, and retailers. During system evolution, materials and information flow between different entities. Each subchain integrates computational agents for coordinated operation. Therefore, such a system is also modeled as a multi-agent one, where information flow, logistics, and node entities create a topological structure (Li *et al*., 2020; Peng *et al*., 2021; Farrera *et al*., 2020). Production and supply chain systems frequently encounter design changes from unforeseen disruptions, including production failures, environmental factors, and equipment malfunctions. These disruptions cause topology changes, resulting in system evolution under switching network structures. Consequently, achieving a consensus of multi-agent based production and supply chain systems is a fundamental task for cooperative control subject to design changes. This implies that all inventory levels converge to the same level under a specific interaction protocol. For instance, in the event of a design change, various components requiring matching are allocated to different factories for production. Conversely, different manufacturers produce the same product based on varying proportion coefficients. This approach facilitates scheduling and distribution, making it easier to mitigate the impact of uncertain customer demand. Several research achievements related to reaching a consensus in production and supply chain systems based on multi-agent approaches have been documented in the literature (see, e.g., Luo *et al*., 2014; Liu *et al.*, 2022; Li *et al*., 2020; González *et al*., 2022). In the work of Bu *et al*. (2019), H_∞ control of a dual-time scale production-inventory system with Markov jump parameters and time-varying delay was studied, and in that of Li *et al*. (2020), H_∞ consensus of a multi-agent based supply chain system was discussed under switching topology and uncertain requirements. These findings confirm that distributed multi-agent control enhances information and material flow across network nodes. However, the existing approaches predominantly assume linear systems with precise mathematical models. The inherent nonlinear characteristics of real production and supply chain systems remain inadequately addressed. Recently, researchers have begun exploring convex control approaches to address the nonlinear characteristics of multi-agent systems (López-Estrada *et al*., 2024), which offers promising insights for nonlinear control of supply chain systems. The extensive input-output data from production and transportation processes makes precise system modeling particularly challenging. Introducing data-driven methods, along with new achievements such as those of Zhao and Yu (2017) or Liang *et al*. (2021), can efficiently address consensus control in actual production and supply chain systems. Recent advances in distributed aggregative optimization (Wang *et al*., 2024) and control-theoretic interpretations of gradient tracking (Notarnicola *et al*., 2023) provide additional tools for addressing these challenges.

The new generation of information technology has transformed modern manufacturing through industrial internet networks. These networks connect enterprises, machines, people, and physical systems, enabling comprehensive sensing, dynamic transmission, and real-time analysis of industrial data. This allows intelligent control and scientific decision-making to enhance efficient allocation of manufacturing resources. Manufacturing systems face inevitable disruptions from uncertainties in both supply chain partners and operational environments. These events may include supply chain blockages or disruptions caused by new outbreaks like the COVID-19 pandemic or trade wars, as well as network collapses resulting from sudden disasters or malicious cyber attacks. Consequently, adapting production and supply chain systems to handle unexpected events has become a critical research priority. This issue has garnered significant attention in recent decades (see, e.g., Wright, 1997; Jarratt *et al*., 2011; Ullah *et al*., 2016; Ivanov *et al*., 2019a). In the engineering community, researchers have extensively studied the issue of design changes from both the production design and supply chain perspectives. For instance, in the works of Wright (1997) and Jarratt *et al*. (2011), overviews of change design on the connotations, causes, processes and contents are systematically summarized, and a dozen studies on change effects propagation are reported in the literature (see, e.g., Eckert *et al*., 2004; Clarkson *et al*., 2004; Ullah *et al*., 2016). On the supply chain side, changes in suppliers and/or demands due to unexpected events such as fires, tsunami, earthquakes, cyber security breaches, or operational factors can significantly alter the supply chain structure and have a profound impact on its performance (Behzadi *et al*., 2018). A large number of studies have investigated the robustness of a network topology through analysis, measurability, and optimization problems (see, e.g., Zhao *et al*., 2019), and the impact of the change effect is reflected as a ripple effect (Ivanov *et al*., 2019b) and a bullwhip effect (Lee *et al*., 2000), etc. Note that, although some studies focus on change design and/or change effects from the production side or supply chain sides, there is a scarcity of research on the collaborative evolution system of the production and supply chain, particularly for data-driven systems using the MFAC approach. In this paper, inspired by the pioneering studies on data-driven control approaches and change design for production and supply chain systems, we are interested in data-driven inventory consensus control for the collaborative evolution system of a production and supply chain subject to design changes. The main contributions of this paper are as follows:

- Under the framework of a multi-agent system, the production and supply chain system is modeled as a multi-agent one. In this model, each node represents a subchain acting as an agent. When a design change occurs, the system undergoes a switch in its topology.
- A digraph data-driven consensus control protocol is proposed to achieve a consensus on inventory levels in production and supply chain systems. The proposed protocol relies on both input/output data of agents and digraph information. The switching topology models the changes in the information flow among enterprises.
- The saturation function is introduced in protocol design to address the issue of productivity limitation that arises when design changes occur.
- The convergence analysis is conducted using the contracting mapping principle, and the efficacy of the proposed data-driven consensus approach is validated through a numerical simulation example.

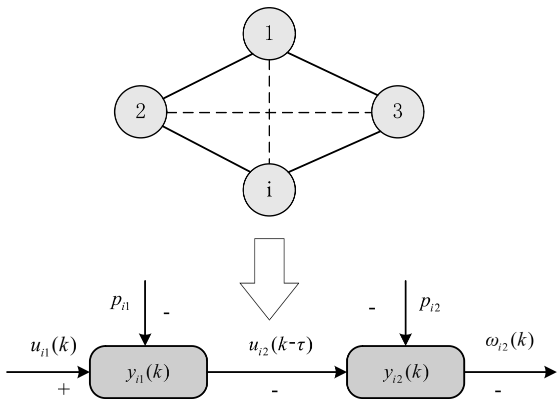

Fig. 1. Supply chain model block diagram.

2. Problem formulation and preliminaries

Let $G = \{V, E, A\}$ describe the directed information interaction topology among multi-agents, where $V = \{1, 2, \dots N\}$, $E \subseteq \{(i,j), i, j \in V\}$ represents the set of vertices and directed edges of a directed graph, while $A = [a_{ij}] \in R^{N\times N}$ denotes the adjacency matrix of the graph when $(j,i) \in E$, $a_{ij} > 0$, otherwise $a_{ij} = 0$. Accordingly, the Laplace matrix of the graph is $L = D - A$, where the first diagonal element of the matrix is $d_i = \sum_{j=1}^{N} a_{ij}$. In addition, the graph $\overline{G}$ is an extended graph of G, which contains N follow nodes and a leader node. Similarly, the diagonal matrix $\boldsymbol{M} = \mathrm{diag}\{o_1, \cdots, o_n\}$ is the adjacency matrix of the leader, with $o_i > 0$ indicating that the agent can receive information from the leader agent, otherwise $o_i = 0$.

Consider a supply chain system with N structurally similar subchains. The i-th subchain, a second-order system, has the logistics and information flow structure shown in Fig. 1. Assume that each factory produces a single product, and the product from the first factory serves as raw material for the second factory. Also $y_{i1}(k)$ represents the inventory level of product 1 of the i-th subchain, and it is assumed that product 1 will be consumed at the rate of p_{i1} over time. Consider the production model of factory 1 in the i-th subchain as follows:

$$y_{i1}(k+1) = (1-p_{i1})y_{i1}(k) + u_{i1}(k) - u_{i2}(k-\tau)\ , \quad (1)$$

where τ is time delay, which means that the production of factory 1 is affected by the control input from factory 2 at time $k - \tau$. This delay may result from the actual transportation time in logistics, information processing time, or communication latency between different stages of the supply chain.

The production model of factory 2 in the i-th subchain is

$$y_{i2}(k+1) = (1-p_{i2})y_{i2}(k) + u_{i2}(k) - \omega_{i2}(k)\ . \quad (2)$$

For external market demand, this model is to generate the required I/O data.

In the actual production process, the supply chain is altered due to uncertain factors such as market customer demand changes, network security issues, trade wars, epidemics, and so on. Therefore, the topology will change. Inventory $y_{ij}(k)$ and productivity $u_{ij}(k)$ are the state variable and control input of the j-th device in the i-th subchain, respectively. Each subchain forms a cascade system, where not only the productivity $u_{ij}(k)$ but also the requirements from subsequent devices influence the system dynamics. Only the final device entity of each subchain is directly affected by market requirements. Market demand uncertainty serves as an external disturbance to the system.

In practical supply chain systems, productivity saturation issues inevitably arise due to production constraints or safety concerns. In order to address the inventory tracking control problem of MIMO nonlinear discrete-time systems with productivity saturation, this section investigates a consistency control method. Specifically, we are considering a MIMO nonlinear discrete-time system with productivity saturation and utilizing the consistency control method to achieve inventory tracking control.

The multi-input multi-output (MIMO) nonlinear supply chain system studied can be expressed as follows:

$$\begin{aligned}\boldsymbol{y}_i(k+1) = \boldsymbol{f}_i(\boldsymbol{y}_i(k),\dots,\boldsymbol{y}_i(k-n_y),\boldsymbol{u}_i(k),\dots,\\ \boldsymbol{u}_i(k-n_u)) + \boldsymbol{\omega}_i(k), \quad i=1,2,\dots,N,\end{aligned} \tag{3}$$

where $\boldsymbol{u_i}(k) \in \boldsymbol{R}^m$ and $\boldsymbol{y_i}(k) \in \boldsymbol{R}^m$ denote the system input and output at time k, respectively, while $n_y, n_u \in Z^+$ are unknown positive integers. The vector $\boldsymbol{\omega}_i(k) = \begin{bmatrix}\omega_{i1}(k) & \cdots & \omega_{im}(k)\end{bmatrix}^T$ represents external disturbances for the i-th subchain at time k, and $\boldsymbol{f}_i(\cdots) = (f_{i1}(\cdots)\cdots f_{im}(\cdots))^T$ denotes unknown nonlinear vector functions.

In this paper, $\boldsymbol{u}_i(k) = \begin{bmatrix}\boldsymbol{u}_{i1}(k) & \cdots & \boldsymbol{u}_{im}(k)\end{bmatrix}^T$, and the saturation function is defined as follows:

$$\bar{\boldsymbol{u}}_i(k) = \begin{bmatrix}\mathrm{Sat}(u_{i1}(k),0,u_{\max})\\ \mathrm{Sat}(u_{i2}(k),0,u_{\max})\\ \vdots\\ \mathrm{Sat}(u_{im}(k),0,u_{\max})\end{bmatrix}, \tag{4}$$

with each component designed as

$$\mathrm{Sat}(u_{ij},0,u_{\max}) = \begin{cases}0, & u_{ij}(k)\le 0,\\ \bar{u}_{ij}(k), & 0<u_{ij}(k)<u_{\max},\\ u_{\max}, & u_{ij}(k)\ge u_{\max},\end{cases} \tag{5}$$

where $j = 1,\cdots,m$ and $\bar{\boldsymbol{u}}_i(k)$ is the output of the controller to be designed, $\bar{u}_{ij}(k)$ is one of the components, while $u_{\max}$ and 0 are the bounds of $u_{ij}(k)$. For the saturation functions (4) and (5), the relation between $\Delta\bar{\boldsymbol{u}}_i(k)$ and $\Delta\boldsymbol{u}_i(k)$ satisfies $\Delta\boldsymbol{u}_i(k) = l_i(k)\Delta\bar{\boldsymbol{u}}_i(k)$, where $\Delta\boldsymbol{u}_i(k) = \boldsymbol{u}_i(k) - \boldsymbol{u}_i(k-1)$ and $\Delta\bar{\boldsymbol{u}}_i(k) = \bar{\boldsymbol{u}}_i(k) - \bar{\boldsymbol{u}}_i(k-1), \boldsymbol{l}(k) = \mathrm{diag}\{l_1(k),\cdots,l_n(k)\}$; from the literature (Bu *et al.*, 2018), $0 \le l_i(k) \le 1, i = 1,\cdots,n$.

Assumption 1. All time-varying switch communication diagrams are strongly connected and the trajectory information of virtual leads can be transmitted directly to one or more follower agents.

Remark 1. The strong connectivity assumption ensures information accessibility between all nodes in the supply chain network. While temporary disconnections may occur in practice, modern supply chain systems typically maintain redundant communication paths. During brief communication interruptions, the system can sustain short-term operations through historical data and predictive mechanisms, ensuring operational continuity.

Assumption 2. For $\boldsymbol{f}_i(\cdots)$, each component with respect to component $(n_y + 2)$ has continuous partial derivatives.

Remark 2. The continuity of partial derivatives reflects the gradual evolution characteristic of supply chain processes. Production, transportation, and inventory management typically evolve progressively rather than abruptly, making this assumption valid in most practical scenarios. This smooth behavior enables reliable system modeling and control design.

Assumption 3. The system (3) satisfy the generalized Lipchitz condition, that is, for each agent with $\|\Delta\boldsymbol{H}_i(k)\| \neq 0$,

$$\|\Delta\boldsymbol{y}_i(k+1)\| \le \kappa\,\|\Delta\boldsymbol{H}_i(k)\|, \tag{6}$$

where $\Delta\boldsymbol{y}_i(k+1) = \boldsymbol{y}_i(k+1) - \boldsymbol{y}_i(k), \Delta\boldsymbol{H}_i(k) = \boldsymbol{H}_i(k) - \boldsymbol{H}_i(k-1)$, $\boldsymbol{H}_i(k) = \boldsymbol{u}_i(k) + \boldsymbol{\omega}_i(k)$, $\boldsymbol{H}_i(0)$ is the initial value of $\boldsymbol{H}_i(k)$, and κ is a constant.

Remark 3. The Lipschitz condition captures the inherent resilience and buffering capacity of real supply chain systems. Market fluctuations and supply disruptions are naturally bounded by physical constraints and safety stock mechanisms. This assumption ensures bounded input–output relationships, which is essential for maintaining system stability and preventing unbounded responses to disturbances.

For the system (3) satisfying Assumptions 2 and 3, if $\|\Delta\boldsymbol{H}_i(k)\| \neq 0$, there exists a time-varying parameter matrix $\boldsymbol{\Phi}_i(k)$ of agent i, called a pseudo Jacobian matrix. The system (3) can be equivalently transformed into the following data model:

$$\Delta\boldsymbol{y}_i(k+1) = \boldsymbol{\Phi}_i(k)\Delta\boldsymbol{H}_i(k), \tag{7}$$

where $\mathbf{\Phi}_i(k) = [\mathbf{\Phi}_{i,1}(k), \mathbf{\Phi}_{i,2}(k)]$, $\|\mathbf{\Phi}_i(k)\| \le b$.

Assumption 4. For all k, $\|\Delta \boldsymbol{H}_i(k)\| \neq 0$, and the signs of all elements of $\mathbf{\Phi}_i(k)$ are unchanged.

Remark 4. The sign invariance of matrix elements holds within short-term local operations, reflecting the relatively stable dynamic characteristics of supply chain systems. While long-term structural changes may occur, the system's fundamental input–output relationships remain consistent over the control horizon, validating this assumption for practical implementation.

3. Main results

3.1. Control protocol design. Consider the following criterion function for control input:

$$\boldsymbol{J}_i(\boldsymbol{u}_i(k)) = \|\Lambda_i(k)\|^2 + \lambda_i \|\Delta \boldsymbol{u}_i(k)\|^2, \tag{8}$$

where

$$\Lambda_i(k) = \sum_{j \in N_i} a_{ij}(\boldsymbol{y}_j(k) - \boldsymbol{y}_i(k+1)) + d_i(\boldsymbol{y}_d(k+1) - \boldsymbol{y}_i(k+1))$$

represents the local consensus error, and the weight factor $\lambda_i > 0$ balances between tracking accuracy and control smoothness. Here, $\boldsymbol{y}_d(k)$ stands for the desired reference trajectory provided by a virtual leader, which guides the inventory levels of all subchains in the multi-agent supply chain system. In practical applications, $\boldsymbol{y}_d(k)$ is determined based on market demand forecasts, seasonal variations, promotional plans, and other business factors.

The term

$$\sum_{j \in N_i} a_{ij}(\boldsymbol{y}_j(k) - \boldsymbol{y}_i(k+1))$$

represents a predictive control strategy where agent i utilizes its neighbors' current inventory levels $\boldsymbol{y}_j(k)$ to determine its next-step inventory $\boldsymbol{y}_i(k+1)$.

This formulation aligns with practical supply chain operations, as nodes typically make decisions based on available information rather than unknown future states. The control input $\boldsymbol{u}_i(k)$ influences $\boldsymbol{y}_i(k+1)$ through system dynamics, creating a natural feedback mechanism.

Remark 5. There are two parts in the control input criterion function (8). The term

$$\sum_{j \in N_i} a_{ij}(\boldsymbol{y}_j(k) - \boldsymbol{y}_i(k+1))$$

in the first part represents the local error between agent i and its neighbors, $d_i(\boldsymbol{y}_d(k+1) - \boldsymbol{y}_i(k+1))$ denotes the error between agent i and its desired reference signal, and term $\lambda_i \|\Delta \boldsymbol{u}_i(k)\|^2$ is the penalty term for not changing the control input too fast.

Notably, in supply chain scenarios, downstream nodes routinely adjust their production plans based on upstream nodes' current inventory levels. The formulation $\boldsymbol{y}_j(k) - \boldsymbol{y}_i(k+1)$ is deliberately chosen over alternatives. Using $\boldsymbol{y}_j(k+1) - \boldsymbol{y}_i(k+1)$ would introduce information coupling and computational complexity, whereas $\boldsymbol{y}_j(k) - \boldsymbol{y}_i(k)$ would eliminate the control input's effect on the optimization objective. The current design both ensures the feasibility of the algorithm and maintains the distributed characteristics of the system.

Let the formation tracking error be defined as $\boldsymbol{e}_i(k) = \boldsymbol{y}_d(k) - \boldsymbol{y}_i(k)$. The distributed formation error for agent i is then defined as

$$\begin{aligned}\boldsymbol{\xi}_i(k) &= \sum_{j \in N_i} a_{ij}(\boldsymbol{y}_j(k) - \boldsymbol{y}_i(k)) + d_i(\boldsymbol{y}_d(k) - \boldsymbol{y}_i(k)) \\ &= \sum_{j \in N_i} a_{ij}(\boldsymbol{y}_j(k) - \boldsymbol{y}_i(k)) + d_i(\boldsymbol{y}_d(k+1) \\ &\quad - \Delta \boldsymbol{y}_d(k+1) - \boldsymbol{y}_i(k)) + d_i \Delta \boldsymbol{y}_d(k+1).\end{aligned} \tag{9}$$

The distributed formation error $\boldsymbol{\xi}_i(k)$ aggregates weighted inventory deviations from neighboring agents through adjacency coefficients a_{ij}. The term d_i indicates whether agent i receives direct information from the virtual leader, while $\Delta \boldsymbol{y}_d(k+1)$ captures the change in the desired reference trajectory. Substituting Eqns. (7) and (9) into the criterion function (8), take the partial derivative with respect to $\boldsymbol{u}_i(k)$ and set it to zero to obtain

$$\begin{aligned}\Delta \boldsymbol{u}_i(k) &= \Big(\lambda_i \boldsymbol{I} + \mathbf{\Phi}_i^T(k)\mathbf{\Phi}_i(k)\Big(\sum_{j \in N_i} a_{ij} + d_i\Big)^2\Big)^{-1} \\ &\quad \times \Big(\sum_{j \in N_i} a_{ij} + d_i\Big)\mathbf{\Phi}_i^T(k) \\ &\quad \times \Big[\boldsymbol{\xi}_i(k) + d_i \Delta \boldsymbol{y}_d(k+1) \\ &\quad - \mathbf{\Phi}_i(k)\Delta \boldsymbol{\omega}_i(k)\Big(\sum_{j \in N_i} a_{ij} + d_i\Big)\Big],\end{aligned} \tag{10}$$

where $j \in N_i$ stands for the neighbor agent of agent i and d_i denotes whether agent i can receive information from leader agent $\boldsymbol{y}_d(k)$.

It is noted that Eqn. (10) requires the inverse operation of the matrix. When the system input-output dimension is large, the inverse operation is very complicated and not easy to be applied in practice. In order to avoid it, the following simplified form is used:

$$\Delta \boldsymbol{u}_i(k) = \frac{\rho_1 \mathbf{\Phi}_i^T(k)\Big(\sum_{j \in N_i} a_{ij} + d_i\Big)\boldsymbol{\xi}_i(k)}{\lambda_i + \Big\|\mathbf{\Phi}_i^T(k)\Big(\sum_{j \in N_i} a_{ij} + d_i\Big)\Big\|^2}$$

$$+\frac{\rho_2\boldsymbol{\Phi}_i^T(k)\Big(\sum\limits_{j\in N_i}a_{ij}+d_i\Big)d_i\Delta\boldsymbol{y}_d(k+1)}{\lambda_i+\left\|\boldsymbol{\Phi}_i^T(k)\Big(\sum\limits_{j\in N_i}a_{ij}+d_i\Big)\right\|^2}-\frac{\rho_3\boldsymbol{\Phi}_i^T(k)\boldsymbol{\Phi}_i(k)\Big(\sum\limits_{j\in N_i}a_{ij}+d_i\Big)^2\Delta\boldsymbol{\omega}_i(k)}{\lambda_i+\left\|\boldsymbol{\Phi}_i^T(k)\Big(\sum\limits_{j\in N_i}a_{ij}+d_i\Big)\right\|^2},\tag{11}$$

where $\rho_l \in (0,1], l = 1,\dots,3$, is the step size factor, which is used to make the control algorithm more general.

The simplified control law (11) incorporates three step-size factors, ρ_1, ρ_2, and ρ_3, which modulate the contributions of consensus tracking, reference following, and disturbance compensation, respectively. The pseudo-Jacobian matrix $\boldsymbol{\Phi}_i(k)$ captures the local input–output relationship of the nonlinear system.

Let us consider the following estimation criterion function:

$$\begin{aligned}&\boldsymbol{J}(\boldsymbol{\Phi}_i(k))\\&=\|\boldsymbol{y}_i(k)-\boldsymbol{y}_i(k-1)-\boldsymbol{\Phi}_i(k)\Delta\boldsymbol{H}_i(k-1)\|^2\\&\quad+\mu\left\|\boldsymbol{\Phi}_i(k)-\hat{\boldsymbol{\Phi}}_i(k-1)\right\|^2.\end{aligned}\tag{12}$$

Taking the partial derivative with respect to $\boldsymbol{\Phi}_i(k)$ and setting it to zero, we can obtain a pseudo-block Jacobi matrix $\boldsymbol{\Phi}_i(k)$ estimation algorithm:

$$\begin{aligned}&\hat{\boldsymbol{\Phi}}_i(k)=\hat{\boldsymbol{\Phi}}_i(k-1)\\&+\frac{\eta(\Delta\boldsymbol{y}_i(k)-\hat{\boldsymbol{\Phi}}_i(k-1)\Delta\boldsymbol{H}_i(k-1))\Delta\boldsymbol{H}_i^T(k-1)}{\mu+\|\Delta\boldsymbol{H}_i(k-1)\|^2},\end{aligned}\tag{13}$$

where $\mu > 0$ is the weight factor, $\eta \in (0,2]$ is the step size factor, and $\hat{\boldsymbol{\Phi}}_i(k) = [\hat{\boldsymbol{\Phi}}_{i,1}(k), \hat{\boldsymbol{\Phi}}_{i,2}(k)]$,

$$\begin{aligned}&\hat{\phi}_{i,1,pp}(k)=\hat{\phi}_{i,1,pp}(1),\text{if }\left|\hat{\phi}_{i,1,pp}(k)\right|<b_2,\\&\text{or }\left|\hat{\phi}_{i,1,pp}(k)\right|>\alpha b_2,\\&\text{or } sign(\hat{\phi}_{i,1,pp}(k))\neq sign(\hat{\phi}_{i,1,pp}(1))\\&\hat{\phi}_{i,1,pq}(k)=\hat{\phi}_{i,1,pq}(1),\text{if }\left|\hat{\phi}_{i,1,pq}(k)\right|>b_1,\\&\text{or } sign(\hat{\phi}_{i,1,pq}(k))\neq\hat{\phi}_{i,1,pq}(1),p\neq q.\end{aligned}\tag{14}$$

The formula (14) is introduced to enable the pseudo-Jacobian matrix estimation algorithm to have a stronger tracking ability of parameter changes.

It is worth noting that, although the optimization of the criterion function (8) only involves local operations, the local extremum problem can be effectively alleviated through the following mechanisms: first, the criterion function has a quadratic structure and exhibits convexity under appropriate conditions; second, the data-driven pseudo-Jacobian matrix estimation algorithm (13) combined with the reset mechanism (14) provides additional robustness guarantees for the system. Finally, the stability analysis in Theorem 1 theoretically proves the boundedness of the system. The synergistic effect of these mechanisms ensures the effectiveness of the proposed method in practical applications.

Based on the control law (11) and the pseudo-block Jacobi matrix estimation algorithm (13), we can derive a data-driven inventory consensus control scheme:

$$\begin{aligned}\bar{\boldsymbol{u}}_i(k)=&\frac{\rho_1\hat{\boldsymbol{\Phi}}_i^T(k)\Big(\sum\limits_{j\in N_i}a_{ij}+d_i\Big)\boldsymbol{\xi}_i(k)}{\lambda_i+\left\|\hat{\boldsymbol{\Phi}}_i^T(k)\Big(\sum\limits_{j\in N_i}a_{ij}+d_i\Big)\right\|^2}\\&+\frac{\rho_2\hat{\boldsymbol{\Phi}}_i^T(k)\Big(\sum\limits_{j\in N_i}a_{ij}+d_i\Big)d_i\Delta\boldsymbol{y}_d(k+1)}{\lambda_i+\left\|\hat{\boldsymbol{\Phi}}_i^T(k)\Big(\sum\limits_{j\in N_i}a_{ij}+d_i\Big)\right\|^2}\\&-\frac{\rho_3\hat{\boldsymbol{\Phi}}_i^T(k)\hat{\boldsymbol{\Phi}}_i(k)\Big(\sum\limits_{j\in N_i}a_{ij}+d_i\Big)^2\Delta\boldsymbol{\omega}_i(k)}{\lambda_i+\left\|\hat{\boldsymbol{\Phi}}_i^T(k)\Big(\sum\limits_{j\in N_i}a_{ij}+d_i\Big)\right\|^2}\\&+\bar{\boldsymbol{u}}_i(k-1).\end{aligned}\tag{15}$$

3.2. Stability analysis.

Theorem 1. *Consider the multi-agent system* (3) *satisfying Assumptions 1–4, and apply the model-free consistency algorithms* (11), (13) *and* (14)*. Then there exists $\lambda_{\min} > 0$, so that when $\lambda > \lambda_{\min}$ the consistency error is bounded and its upper bound is satisfied:*

$$\begin{aligned}&\|\boldsymbol{E}(k)\|\leq\left\|[(\boldsymbol{L}+\boldsymbol{D})\otimes\boldsymbol{I}_m]^{-1}\boldsymbol{\xi}_i(k)\right\|,\\&\|\boldsymbol{\xi}_i(k)\|\\&\leq\frac{\sum\limits_{j\in N_i}a_{ij}b+2\|\Delta\boldsymbol{y}_d(k)\|+\Big(\sum\limits_{j\in N_i}a_{ij}+d_i\Big)b}{1-\bar{d}_M}M_1\\&\quad+\frac{b\bar{b}M_1\Big(\sum\limits_{j\in N_i}a_{ij}+d_i\Big)^2}{(1+\bar{d}_M)\sqrt{\lambda_{\min}}},\end{aligned}\tag{16}$$

where $\boldsymbol{\xi}(k) = [{\boldsymbol{\xi}_1}^T(k),\dots,{\boldsymbol{\xi}_N}^T(k)]^T$ is the local adjacency error of all nodes, while $M_1, \bar{d}_M$ and $\lambda_{\min}$ are the constants that satisfy (22)*,* (29)*,* (33)*, respectively.*

Proof. From the definitions of (9) and $\boldsymbol{e}_i(k)$, we can obtain

$$\begin{aligned}\boldsymbol{\xi}_i(k) &= \sum_{j\in N_i} a_{ij}(\boldsymbol{y}_j(k)-\boldsymbol{y}_i(k)) + d_i(\boldsymbol{y}_d(k)-\boldsymbol{y}_i(k))\\ &= \sum_{j\in N_i} a_{ij}(\boldsymbol{e}_i(k)-\boldsymbol{e}_j(k)) + d_i\boldsymbol{e}_i(k).\end{aligned} \tag{17}$$

From (16) it can be derived that

$$\boldsymbol{\xi}(k) = [(\boldsymbol{L}+\boldsymbol{D})\otimes \boldsymbol{I}_m]\boldsymbol{E}(k). \tag{18}$$

The directed graph $\boldsymbol{G}$ contains a spanning tree, so $\boldsymbol{L}+\boldsymbol{D}$ is nonsingular, hence the inverse of $\boldsymbol{L}+\boldsymbol{D}$ and $[(\boldsymbol{L}+\boldsymbol{D})\otimes\boldsymbol{I}_m]$ exists. $\boldsymbol{L}, \boldsymbol{D}, \boldsymbol{I}_m$ are constant matrices, so the norm of $[(\boldsymbol{L}+\boldsymbol{D})\otimes\boldsymbol{I}_m]^{-1}$ is bounded. $\|\boldsymbol{E}(k)\| \le \left\|[(\boldsymbol{L}+\boldsymbol{D})\otimes\boldsymbol{I}_m]^{-1}\right\| \|\boldsymbol{\xi}(k)\|$, so the boundedness of $\boldsymbol{\xi}(k)$ guarantees that of $\boldsymbol{E}(k)$, and then we show that $\boldsymbol{\xi}_i(k)$ is bounded. Now, substitute (7) into (9) to calculate the relationship between $\boldsymbol{\xi}_i(k)$ and $\boldsymbol{\xi}_i(k-1)$:

$$\begin{aligned}\boldsymbol{\xi}_i(k) &= \sum_{j\in N_i} a_{ij}(\boldsymbol{y}_j(k)-\boldsymbol{y}_i(k)) + d_i(\boldsymbol{y}_d(k)-\boldsymbol{y}_i(k))\\ &= \boldsymbol{\xi}_i(k-1) + \Delta\boldsymbol{\xi}_i(k)\\ &= \boldsymbol{\xi}_i(k-1) + \sum_{j\in N_i} a_{ij}\boldsymbol{\Phi}_j(k-1)\Delta\boldsymbol{H}_j(k-1)\\ &\quad - \Big(\sum_{j\in N_i} a_{ij}+d_i\Big)\boldsymbol{\Phi}_i(k-1)[\Delta\boldsymbol{u}_i(k-1)\\ &\quad \Delta\boldsymbol{\omega}_i(k-1)] + d_i\Delta\boldsymbol{y}_d(k).\end{aligned} \tag{19}$$

Let us substitute (15) into (19) to get

$$\begin{aligned}&\boldsymbol{\xi}_i(k) =\\ &\left[\boldsymbol{I}_m - \frac{\rho_1\boldsymbol{\Phi}_i(k-1)\hat{\boldsymbol{\Phi}}_i^T(k-1)\Big(\sum\limits_{j\in N_i} a_{ij}+d_i\Big)^2}{\lambda_i + \left\|\hat{\boldsymbol{\Phi}}_i^T(k-1)\Big(\sum\limits_{j\in N_i} a_{ij}+d_i\Big)\right\|^2}\right]\\ &\times \boldsymbol{\xi}_i(k-1) + \boldsymbol{g}_i(k),\end{aligned} \tag{20}$$

where

$$\begin{aligned}&\boldsymbol{g}_i(k) = \sum_{j\in N_i} a_{ij}\boldsymbol{\Phi}_j(k-1)\Delta\boldsymbol{H}_j(k-1)\\ &-\left[\frac{\rho_2\Big(\sum\limits_{j\in N_i} a_{ij}+d_i\Big)^2 d_i\boldsymbol{\Phi}_i(k-1)\hat{\boldsymbol{\Phi}}_i^T(k-1)}{\lambda_i + \left\|\hat{\boldsymbol{\Phi}}_i^T(k-1)\Big(\sum\limits_{j\in N_i} a_{ij}+d_i\Big)\right\|^2} - d_i\boldsymbol{I}_m\right]\\ &\times\Delta\boldsymbol{y}_d(k) - \Big(\sum_{j\in N_i} a_{ij}+d_i\Big)\hat{\boldsymbol{\Phi}}_i(k-1)\Delta\boldsymbol{\omega}_i(k-1)\\ &+\left[\frac{\rho_3\Big(\sum\limits_{j\in N_i} a_{ij}+d_i\Big)^3\boldsymbol{\Phi}_i(k-1)\hat{\boldsymbol{\Phi}}_i^T(k-1)\hat{\boldsymbol{\Phi}}_i(k-1)}{\lambda_i + \left\|\hat{\boldsymbol{\Phi}}_{i,1}(k-1)\Big(\sum\limits_{j\in N_i} a_{ij}+d_i\Big)\right\|^2}\right]\\ &\times\Delta\boldsymbol{\omega}_i(k-1).\end{aligned} \tag{21}$$

Next, we analyze the boundedness of $\Delta\boldsymbol{H}_j(k-1)$.

Transform the boundedness analysis problem of $\Delta\boldsymbol{H}_j(k-1)$ for any j into the boundedness analysis problem of $\Delta\boldsymbol{H}_i(k)$ for any subchain i and any k.

To simplify the subsequent analysis, we rearrange the elements in $\Delta\boldsymbol{H}_i(k)$ to obtain an augmented matrix $\Delta\boldsymbol{G}_i(k) = \begin{bmatrix}\Delta\boldsymbol{u}_i^T(k), & \Delta\boldsymbol{\omega}_i^T(k)\end{bmatrix}^T$. If the norm of the augmented matrix $\Delta\boldsymbol{G}_i(k)$ is bounded, then it follows that $\|\Delta\boldsymbol{G}_i(k)\| \ge \max\{\|\Delta\boldsymbol{u}_i^T(k)\|, \|\Delta\boldsymbol{\omega}_i^T(k)\|\}$. Therefore, if $\Delta\boldsymbol{G}_i(k)$ is bounded, then the norms of both $\Delta\boldsymbol{u}_i^T(k)$ and $\Delta\boldsymbol{\omega}_i^T(k)$ are bounded; by the triangle inequality, $\Delta\boldsymbol{u}_i^T(k) + \Delta\boldsymbol{\omega}_i^T(k)$ must also be bounded. Since rearranging the elements does not affect the boundedness of the matrix norm, $\Delta\boldsymbol{H}_i(k) = \Delta\boldsymbol{u}_i(k) + \Delta\boldsymbol{\omega}_i(k)$ is bounded.

Step 1. The first step, when $k_1 = 0$, $\Delta\boldsymbol{G}_i(0) = [\Delta\boldsymbol{u}_i^T(0), \Delta\boldsymbol{\omega}_i^T(0)]^T$, is clearly bounded. Without loss of generality,

$$\|\Delta\boldsymbol{G}_i(0)\| \le M_1, \tag{22}$$

and $M_1 > 1$, otherwise let $\bar{M}_1 = 1 + M_1$ be the new upper bound on $\Delta\boldsymbol{G}_i(0)$.

Step 2. For any $k_1 = 1,\dots,k-1$ and $i = 1,\dots,N$, assume $\|\Delta\boldsymbol{G}_i(k_1)\| \le M_1$.

Step 3. Based on the assumptions of Step 2, only the proof $\|\Delta\boldsymbol{G}_i(k)\| \le M_1, i = 1,\dots,N$, is needed, and it can be obtained by substituting (15) for $\Delta\boldsymbol{H}_i(k)$:

$$\Delta\boldsymbol{G}_i(k_1) = \boldsymbol{A}_1(k)[\Delta\boldsymbol{u}_i^T(k), \Delta\boldsymbol{\omega}_i^T(k)]^T + \boldsymbol{\chi}, \tag{23}$$

where

$$\boldsymbol{A}_1(k) = \begin{bmatrix} 0 & \dfrac{-\rho_3\hat{\boldsymbol{\Phi}}_i^T(k)\hat{\boldsymbol{\Phi}}_i(k)\Big(\sum\limits_{j\in N_i} a_{ij}+d_i\Big)^2}{\lambda + \left\|\hat{\boldsymbol{\Phi}}_i^T(k-1)\Big(\sum\limits_{j\in N_i} a_{ij}+d_i\Big)\right\|^2}\\ \boldsymbol{I}_m & 0\end{bmatrix} \tag{24}$$

and

$$\boldsymbol{\chi} = \left[0, \frac{\hat{\boldsymbol{\Phi}}_i^T(k)(\sum\limits_{j\in N_i} a_{ij}+d_i)(\rho_1\boldsymbol{\xi}_i(k) + d_i\rho_2\Delta\boldsymbol{y}_d(k))}{\lambda + \left\|\hat{\boldsymbol{\Phi}}_i^T(k-1)(\sum\limits_{j\in N_i} a_{ij}+d_i)\right\|^2}\right]^T. \tag{25}$$

Given the known disturbance from external market demand, there exists $\boldsymbol{\sigma}_i(k)$ such that $\boldsymbol{\omega}_i(k) = \boldsymbol{\sigma}_i(k)\boldsymbol{\omega}_i(k-1)$,

$$\Delta \boldsymbol{G}_i(k_1) = \boldsymbol{A}_1(k)\boldsymbol{B}_1(k-1) + \boldsymbol{\chi}, \tag{26}$$

where $\boldsymbol{B}_1(k-1) = [\boldsymbol{\Phi}_i(k), \boldsymbol{\sigma}_i(k)]^T$.

Taking the norm of both sides of Eqn. (26) yields

$$\Delta \boldsymbol{G}_i(k) \le \frac{1}{2}\Delta \boldsymbol{G}_i(k-1) + \|\boldsymbol{\chi}\| \ \le\ \frac{1}{2}M_1 + \|\boldsymbol{\chi}\|. \tag{27}$$

Next, we need to prove that $\|\boldsymbol{\chi}\| \le \frac{1}{2}M_1$:

$$\begin{aligned}\|\boldsymbol{g}_i(k)\| &\le \sum_{j\in N_i} a_{ij}\, b\, M_1 \ +\ 2\, M_1 \,\|\Delta \boldsymbol{y}_d(k)\| \\ &+ \left[\frac{\Big(\sum\limits_{j\in N_i} a_{ij}+d_i\Big)^2}{\sqrt{\lambda}}\, b\,\bar{b} \ +\ \Big(\sum_{j\in N_i} a_{ij}+d_i\Big)\, b\right] M_1 \\ &:= h(M_1,\lambda).\end{aligned} \tag{28}$$

The contraction coefficient $\bar{d}_M \in (0,1)$ measures how rapidly the consensus error diminishes at each iteration. A smaller $\bar{d}_M$ indicates faster convergence. We can find such $\bar{d}_M < 1$ because the control gain sufficiently dampens the error dynamics:

$$\left\| \boldsymbol{I}_m - \frac{\rho_1 \boldsymbol{\Phi}_i(k-1)\hat{\boldsymbol{\Phi}}_i^T(k-1)\Big(\sum\limits_{j\in N_i} a_{ij}+d_i\Big)^2}{\lambda + \left\|\hat{\boldsymbol{\Phi}}_i^T(k-1)\Big(\sum\limits_{j\in N_i} a_{ij}+d_i\Big)\right\|^2} \right\| \le \bar{d}_M < 1. \tag{29}$$

Taking the norm of Eqn. (19) and following Eqns. (28) and (29), we obtain

$$\begin{aligned}\|\boldsymbol{\xi}_i(k)\| &\le \bar{d}_M \,\|\boldsymbol{\xi}_{\mathrm{i}}(k-1)\| + h(M_1,\lambda) \\ &\le \bar{d}_M^2 \,\|\xi_{\mathrm{i}}(k-2)\| + \bar{d}_M h(M_1,\lambda) + h(M_1,\lambda) \\ &\le \cdots \le \bar{d}_M^k \,\|\boldsymbol{\xi}_{\mathrm{i}}(0)\| + \frac{1}{1-\bar{d}_M} h(M_1,\lambda).\end{aligned} \tag{30}$$

According to (24) and (27), we can derive

$$\begin{aligned}\|\boldsymbol{\chi}\| &= \left\| \frac{\hat{\boldsymbol{\Phi}}_i^T(k)\Big(\sum\limits_{j\in N_i} a_{ij}+d_i\Big)\rho_1\boldsymbol{\xi}_i(k)}{\lambda + \left\|\hat{\boldsymbol{\Phi}}_i^T(k-1)\Big(\sum\limits_{j\in N_i} a_{ij}+d_i\Big)\right\|^2} \right\| \\ &\le \frac{\|\boldsymbol{\xi}_i(k)\|}{2\sqrt{\lambda}} \le \frac{h(M_1,\lambda)}{2(1-\bar{d}_M)\sqrt{\lambda}} \\ &= \frac{\sum\limits_{\mathrm{j}\in N_i} a_{ij}b + 2\,\|\Delta \boldsymbol{y}_d(k)\| + \Big(\sum\limits_{j\in N_i} a_{ij}+d_i\Big)b}{2(1-\bar{d}_M)\sqrt{\lambda}} M_1 \\ &+ \frac{b\bar{b}M_1\Big(\sum\limits_{j\in N_i} a_{ij}+d_i\Big)^2}{2(1-\bar{d}_M)\lambda}.\end{aligned} \tag{31}$$

To satisfy $\|\boldsymbol{\chi}\| \le \frac{1}{2}\mathrm{M}_1$, just choose λ so that

$$\begin{aligned}&\frac{\sum\limits_{\mathrm{j}\in N_i} a_{ij}b + 2\,\|\Delta \boldsymbol{y}_d(k)\| + \Big(\sum\limits_{j\in N_i} a_{ij}+d_i\Big)b}{2(1-\bar{d}_M)\sqrt{\lambda}} M_1 \\ &+ \frac{b\bar{b}M_1(\sum\limits_{j\in N_i} a_{ij}+d_i)^2}{2(1-\bar{d}_M)\lambda} \le \frac{1}{2}M_1.\end{aligned} \tag{32}$$

The above equation is obviously true. The threshold $\lambda_{\min}$ represents the minimum control effort required to overcome system uncertainties and ensure convergence. When $\lambda > \lambda_{\min}$, the control action dominates disturbances and coupling effects, guaranteeing that

$$\begin{aligned}\lambda &> \lambda_{\min} \\ &\ge \Big(\frac{b + \sqrt{b^2 + 4(1-d_2)b\bar{b}\Big(\sum\limits_{j\in N_i} a_{ij}+d_i\Big)^2}}{2(1-\bar{d}_M)}\Big)^2.\end{aligned} \tag{33}$$

Hence, statement $\|\Delta \boldsymbol{G}_i(k)\| \le M_1$ is true for any $k = 0, 1, 2, \ldots, i = 1, \ldots, N$.

Then, combine (27), (30) and $\lambda > \lambda_{\min}$ to obtain

$$\begin{aligned}&\|\boldsymbol{\xi}_i(k)\| \\ &\le \frac{\sum\limits_{\mathrm{j}\in N_i} a_{ij}b + 2\,\|\Delta \boldsymbol{y}_d(k)\| + \Big(\sum\limits_{j\in N_i} a_{ij}+d_i\Big)b}{1-\bar{d}_M} M_1 \\ &+ \frac{b\bar{b}M_1\Big(\sum\limits_{j\in N_i} a_{ij}+d_i\Big)^2}{(1-\bar{d}_M)\sqrt{\lambda_{\min}}}.\end{aligned} \tag{34}$$

Since a_{ij}, b, M_1, d_2, d_i are all fixed constants, $\boldsymbol{\xi}_i(k)$ is bounded for all i. It follows from (26) that $\boldsymbol{E}$(k) is bounded. ■

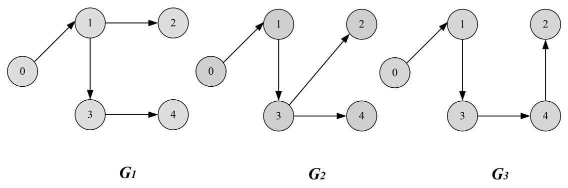

Fig. 2. Switching topology.

4. Simulation study

The product consumption rate is $p_{11} = 0.1$, $p_{12} = 0.2$, $p_{21} = 0.2$, $p_{22} = 0.1$, $p_{31} = 0.2$, $p_{32} = 0.1$, $p_{41} = 0.3$, $p_{42} = 0.1$. The initial conditions are set as $\boldsymbol{u}_i(1) = \begin{bmatrix}1 & 1\end{bmatrix}$, $\boldsymbol{y}_i(1) = \begin{bmatrix}1 & 2\end{bmatrix}$. The parameters of the algorithm are selected as $\tau = 1$, $\rho_1 = \rho_2 = \rho_3 = 0.1$, $\lambda_1 = 0.7$, $\lambda_2 = 0.1$, $\lambda_3 = 0.3$, $\lambda_4 = 0.2$, $\mu = 1$, $\eta = 1$, $\boldsymbol{\Phi}_i(1) = \begin{bmatrix}0.5 & 0\\ 0 & 0.5\end{bmatrix}$.

The switching topology is shown in Fig. 2: when $k = 200$, G_1 is switched to G_2; when $k = 550$, G_2 is switched to G_3; when $k = 700$, G_3 is switched to G_1.

To verify the effectiveness of the proposed method, we compared it with incremental PID control (IPIDC), a classical control strategy that offers relatively stable performance and lower computational complexity. The PID controller parameters are set as $K_p = 0.1$, $K_i = 0.01$, $K_d = 0.03$.

To demonstrate the effectiveness of our proposed method under various market conditions, we designed $\boldsymbol{y}_d(k)$ to incorporate different demand patterns, as shown in Eqn. (35). These patterns include step functions for sudden demand changes, ramp functions for gradual demand shifts, sinusoidal functions for seasonal variations, and constant values for stable demand periods,

$$y_{d1}(k) = y_{d2}(k) = \begin{cases} 0.55 + 0.2\cos(\pi k/100), \\ \quad + 0.25\sin(\pi k/100), k < 400, \\ 0.75, 400 \le k < 470, \\ 0.0035k - 0.9, 470 \le k < 600, \\ 1.2, 600 \le k < 800, \\ 0.1 + e^{-k+800}, 800 \le k < 1000. \end{cases} \tag{35}$$

The external demand disturbances present in the subchains of the multi-agent supply chain system are illustrated in Fig. 3. The supply chain inventory status under data-driven inventory consensus control (DDICC) is shown in Figs. 4 and 5.

As shown in those figures, topology switching at 200, 550, and 700 causes oscillations in states $y_{i1}(k)$ and $y_{i2}(k)$ before convergence to steady-state behavior. The inventory state of each subchain converges to the desired trajectory of the virtual leader. The supply chain inventory status under IPIDC is shown in Figs. 6 and 7.

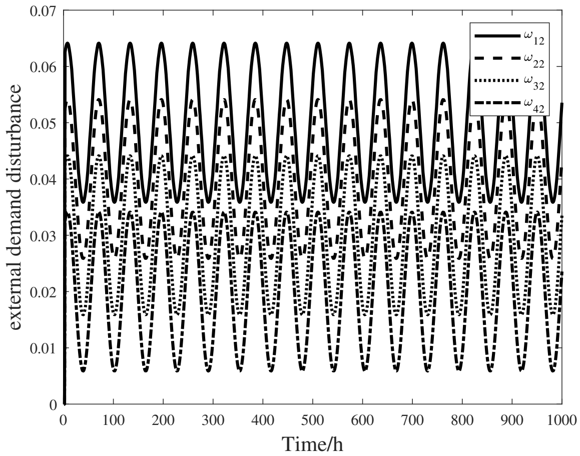

Fig. 3. External demand disturbance.

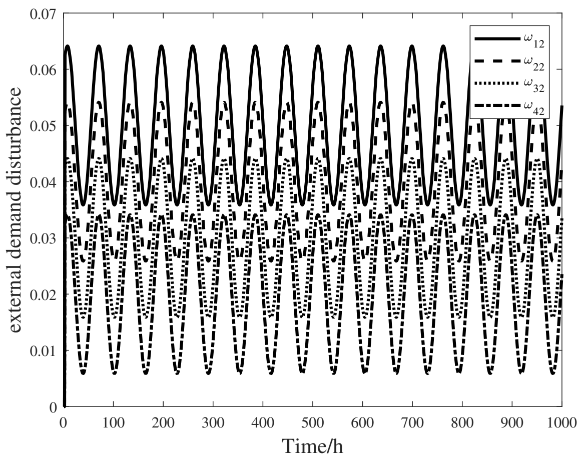

Fig. 4. Supply chain inventory $\boldsymbol{y}_{i1}(k)$ under DDICC.

Compared to Fig. 4, Fig. 6 exhibits larger initial deviations and oscillations. Although the trajectories gradually converge to the desired state, the oscillation amplitude remains larger than that in Fig. 4, and there is a certain degree of inconsistency. Thus, Fig. 6 shows inferior dynamic performance and tracking accuracy compared to Fig. 4. In contrast to Fig. 5, Fig. 7 exhibits larger initial deviations, significant oscillation amplitudes, and slower attenuation, resulting in greater tracking errors. The control algorithm requires further optimization to enhance response speed and dynamic performance. In contrast, Fig. 5 demonstrates faster convergence in the initial phase, smaller oscillation amplitudes during the intermediate phase, and significantly improved system stability and tracking accuracy.

The evolution of inventory tracking errors in

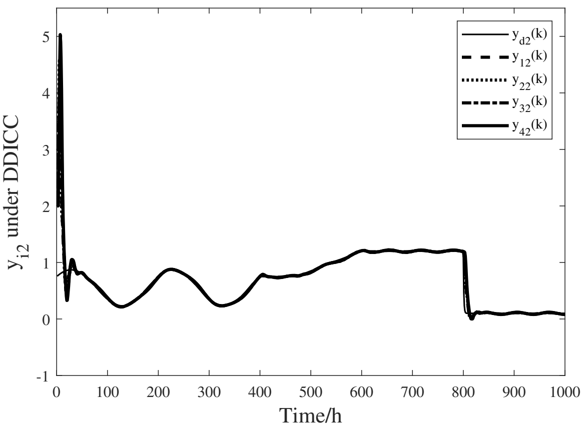

Fig. 5. Supply chain inventory $\boldsymbol{y}_{i2}(k)$ under DDICC.

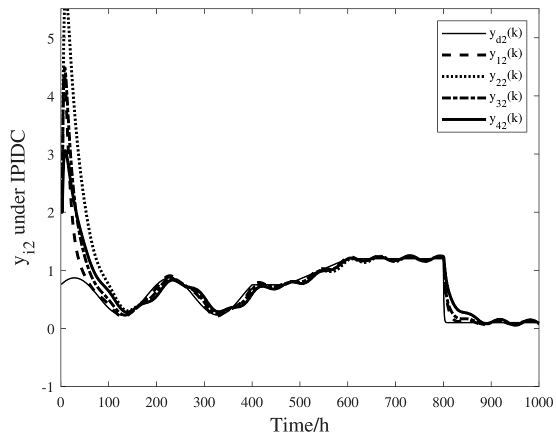

Fig. 7. Supply chain inventory $\boldsymbol{y}_{i2}(k)$ under IPIDC.

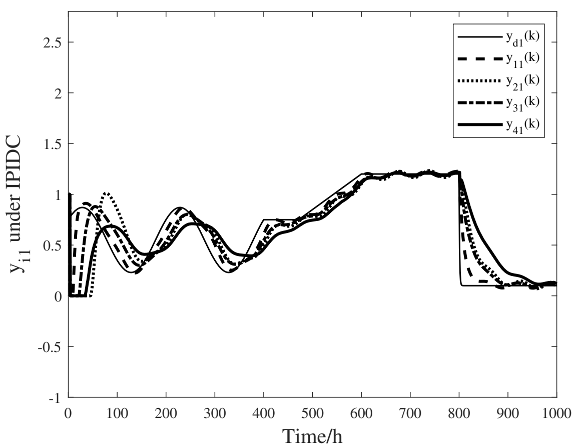

Fig. 6. Supply chain inventory $\boldsymbol{y}_{i1}(k)$ under IPIDC.

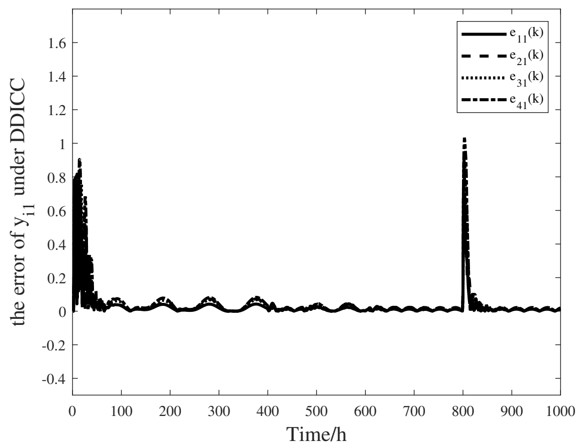

Fig. 8. Tracking error $\boldsymbol{y}_{i1}(k)$ under DDICC.

subchains of the supply chain under DDICC is shown in Figs. 8 and 9.

Figures 8 and 9 show that all errors exhibit rapid decay in the initial stage, indicating that the system can quickly adjust errors and achieve satisfactory dynamic response performance. Furthermore, all tracking errors remain nearly stable at levels close to zero during the subsequent steady-state phase, demonstrating that the system exhibits high precision in this phase and effectively tracks the target inventory levels. Additionally, the consistent behavior of the errors over most of the time period suggests that the system maintains good overall coordination, and the control strategies among different variables are effective.

The tracking errors in subchains of the supply chain under IPIDC are shown in Figs. 10 and 11.

As observed from Figs. 8 and 9 as well as 10 and 11, DDICC demonstrates superior tracking performance compared to IPIDC in terms of error convergence, stability, and disturbance rejection, exhibiting overall better control effectiveness.

In order to quantitatively analyze the effect of the method, the mean absolute error (MAE) was defined as

$$MAE = \frac{1}{\mathrm{T}} \sum_{k=1}^{N} |\boldsymbol{y}_d(k) - \boldsymbol{y}_i(k)|. \tag{36}$$

As shown in Table 1, the MAE values of DDICC are significantly lower than those of IPIDC across all metrics, indicating that the data-driven method is capable of maintaining a consistently low error level. In contrast, IPIDC exhibits larger errors, reflecting its weaker control performance over the system. Furthermore, the performance of DDICC is relatively consistent across all error metrics (MAE values ranging from 0.0354 to 0.0492), whereas IPIDC shows a wider range of error variations (MAE values from 0.0950 to 0.2547). This suggests that DDICC demonstrates stronger robustness under varying conditions.

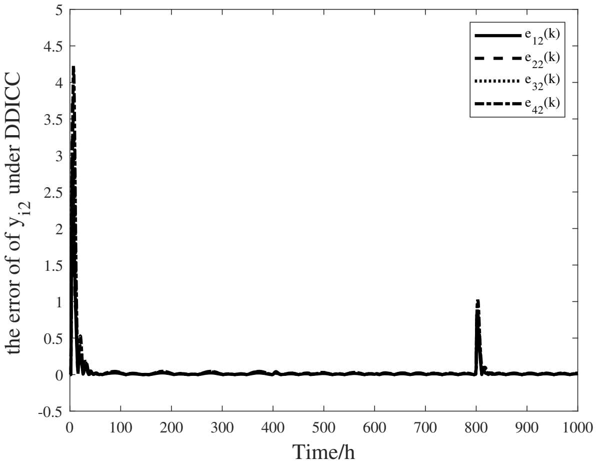

Fig. 9. Tracking error $\boldsymbol{y}_{i2}(k)$ under DDICC.

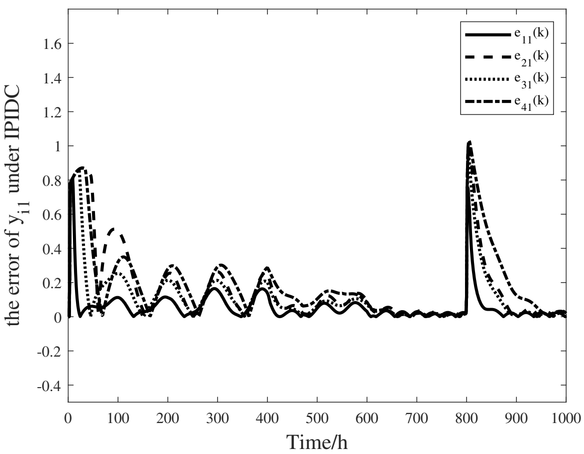

Fig. 10. Tracking error $\boldsymbol{y}_{i1}(k)$ under IPIDC.

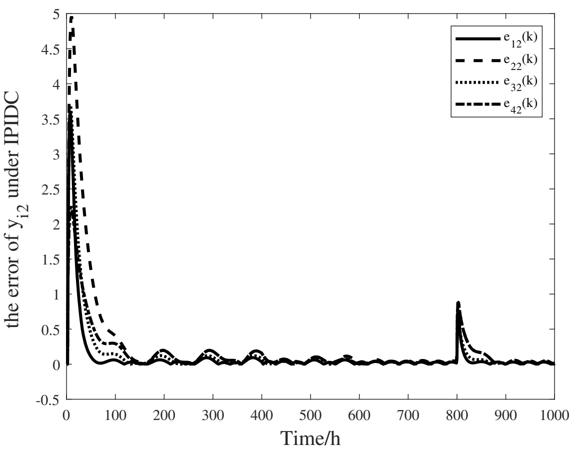

Fig. 11. Tracking error $\boldsymbol{y}_{i2}(k)$ under IPIDC.

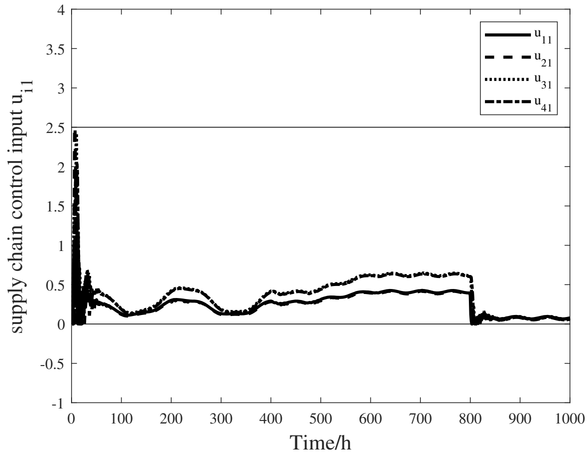

Fig. 12. Supply chain control input $\boldsymbol{u}_{i1}(k)$ under DDICC.

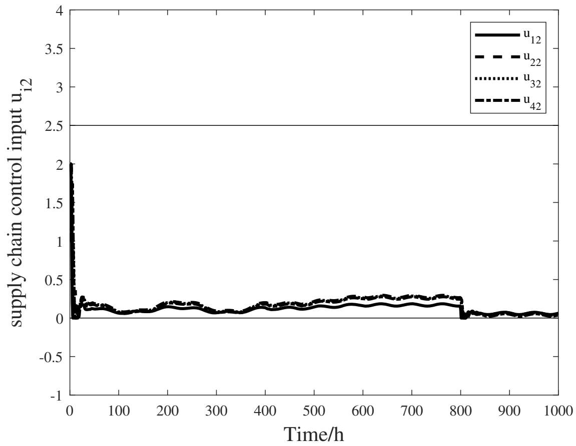

Fig. 13. Supply chain control input $\boldsymbol{u}_{i2}(k)$ under DDICC.

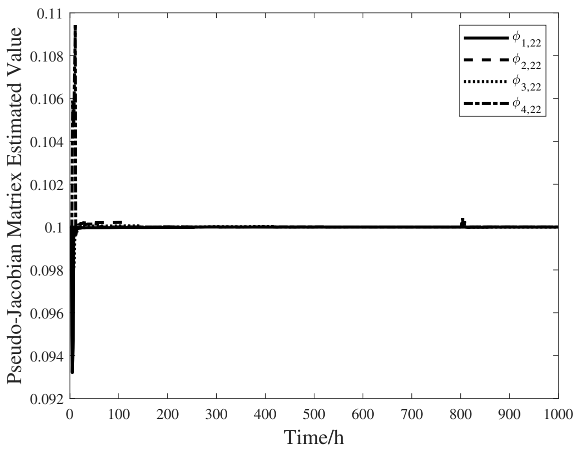

Fig. 14. Estimated PJM.

The supply chain control input under DDICC is shown in Figs. 12 and 13.

According to those figures an input saturation function is added to limit productivity to the range of 0 to 2.5, thus solving the problem of productivity first in the production process. Meanwhile, we can conclude that DDICC with the inclusion of the saturation function addresses the consensus control of the supply chain system under productivity constraints.

Figure 14 illustrates the temporal evolution of the estimated values of the pseudo-Jacobian matrix under DDICC. This figure supports Assumption 4, which posits the invariance of the sign of the pseudo-Jacobian matrix elements.

Let us add time delay $\tau = 0$ and $\tau = 2$. Here, τ is information delay, which is a nonlinear factor in the supply chain system. As DDICC is adopted and does not rely on the model of the system, it can be seen from Table 2 that there is almost no change in the simulation of supply chain system $\tau = 0$ or $\tau = 2$. This shows the validity of the data-driven consistency algorithm.

This study also conducted a sensitivity analysis of the proposed control scheme under different topology switching frequencies. The experimental results, presented in Table 3, demonstrate that, under high-frequency switching conditions (every 100 time steps), the system achieved an average MAE of 0.0459, with subchain tracking errors showing slight increases while maintaining overall stability. Medium-frequency switching ($k = 200, 550, 700$), which served as the primary research configuration in this study, yielded an average MAE of 0.0445, with well-balanced error metrics across all indicators and the system exhibiting strong consensus tracking performance. Under low-frequency switching conditions, the average MAE improved to 0.0433, indicating enhanced performance. The MAE varied by only 6.0% between high-frequency and low-frequency switching, which demonstrates the robust nature of the proposed DDICC algorithm against topological dynamics and its ability to maintain stable control performance across different network configurations.

Table 1. MAE for two methods.

Algorithms	$e_{12}(k)$	$e_{22}(k)$	$e_{32}(k)$	$e_{42}(k)$
DDICC	0.0354	0.0492	0.0450	0.0484
IPIDC	0.0950	0.2547	0.1334	0.1546

Table 2. MAE for different time-delays.

Time-delay	$e_{12}(k)$	$e_{22}(k)$	$e_{32}(k)$	$e_{42}(k)$
$\tau = 0$	0.0339	0.0486	0.0439	0.0480
$\tau = 1$	0.0354	0.0492	0.0450	0.0484
$\tau = 2$	0.0360	0.0525	0.0463	0.0504

Table 3. MAE for different topology switching periods.

Switching times	$e_{12}(k)$	$e_{22}(k)$	$e_{32}(k)$	$e_{42}(k)$
Every 100 steps	0.0368	0.0506	0.0463	0.0498
200,550,700	0.0354	0.0492	0.0450	0.0484
400,800	0.0342	0.0479	0.0438	0.0471

5. Conclusions

This paper presented a data-driven consensus control protocol for supply chain inventory management by transforming an unknown MIMO nonlinearity into an equivalent data model through dynamic linearization technology. The incorporation of a saturation function effectively addresses productivity limitations during unexpected events such as equipment failures or demand surges. The proposed method demonstrates a particular value in automotive parts distribution networks, where multi-tier suppliers must maintain synchronized inventory levels despite frequent production changes and just-in-time delivery constraints. Similarly, in pharmaceutical cold chain logistics, the approach ensures coordinated inventory management across temperature-controlled facilities while handling disruptions from equipment malfunctions or route changes. The key advantage lies in the protocol's reliance solely on I/O data from the multi-agent supply chain system, eliminating complex mathematical modeling requirements while maintaining robust performance under topology switching. This data-driven characteristic enables rapid deployment in existing supply chain infrastructures, reducing implementation costs and improving service levels through enhanced inventory coordination and decreased stockout occurrences, making it particularly suitable for modern supply chains facing dynamic market conditions and diverse stakeholder interactions.

Acknowledgment

This research was funded by the National Key Research and Development Program of China under the grant 2023YFB4604704 and the Project of Cultivation for Young Top-Notch Talents of Beijing Municipal Institutions under the grant BPHR202203231.

References

Ahn, H.S., Chen, Y. and Moore, K.L. (2007). Iterative learning control: Brief survey and categorization, *IEEE Transactions on Systems, Man, and Cybernetics C: Applications and Reviews* **37**(6): 1099–1121, DOI: 10.1109/TSMCC.2007.905759.

Behzadi, G., Sullivan, M.J.O., Olsen, T. and Zhang, A. (2018). Allocation flexibility for agribusiness supply chains under market demand disruption, *International*

Journal of Production Research **56**(10): 3524–3546, DOI: 10.1080/00207543.2017.1349955.

Bu, X., Wang, Q., Hou, Z. and Qian, W. (2018). Data driven control for a class of nonlinear systems with output saturation, *ISA Transactions* **81**: 1–7, DOI: 10.1016/j.isatra.2018.07.009.

Bu, X., Yu, Q., Hou, Z. and Qian, W. (2019). Model free adaptive iterative learning consensus tracking control for a class of nonlinear multiagent systems, *IEEE Transactions on Systems, Man & Cybernetics: Systems* **49**(4): 677–686, DOI: 10.1109/TSMC.2017.2734799.

Chan, F.T. and Zhang, T. (2011). The impact of collaborative transportation management on supply chain performance: A simulation approach, *Expert Systems with Applications* **38**(3): 2319–2329, DOI:10.1016/j.eswa.2010.08.020.

Chi, R., Wang, D., Hou, Z. and Jin, S. (2012). Data-driven optimal terminal iterative learning control, *Journal of Process Control* **22**(10): 2026–2037.

Clarkson, P.J., Simons, C. and Eckert, C. (2004). Predicting change propagation in complex design, *Journal of Mechanical Design* **126**(5): 788–797, DOI:10.1115/1.1765117.

Clempner, J.B. and Poznyak, A.S. (2023). Computing a mechanism for a Bayesian and partially observable Markov approach, *International Journal of Applied Mathematics and Computer Science* **33**(3): 463–478, DOI: 10.34768/amcs-2023-0034.

Coopmans, I., Bijttebier, J., Marchand, F., Mathijs, E., Messely, L., Rogge, E., Sanders, A. and Wauters, E. (2021). COVID-19 impacts on flemish food supply chains and lessons for agri-food system resilience, *Agricultural Systems* **190**: 103136, DOI: 10.1016/j.agsy.2021.103136.

Darmawan, A., Wong, H., Thorstenson, A. and Talley, W. (2021). Supply chain network design with coordinated inventory control, *Transportation Research E: Logistics and Transportation Review* **145**: 102168, DOI: 10.1016/j.tre.2020.102168.

Eckert, C., Clarkson, P.J. and Zanker, W. (2004). Change and customisation in complex engineering domains, *Research in Engineering Design* **15**(1): 1–21, DOI:10.1007/s00163-003-0031-7.

Farrera, B., López-Estrada, F.-R., Chadli, M., Valencia-Palomo, G. and Gómez-Peñate, S. (2020). Distributed fault estimation of multi-agent systems using a proportional-integral observer: A leader-following application, *International Journal of Applied Mathematics and Computer Science* **30**(3): 551–560, DOI: 10.34768/amcs-2020-0040.

Ge, S.S., Hang, C.C., Lee, T.H. and Zhang, T. (2013). *Stable Adaptive Neural Network Control*, Springer Science & Business Media, New York.

Gomi, H. and Kawato, M. (1993). Neural network control for a closed-loop system using feedback-error-learning, *Neural Networks* **6**(7): 933–946, DOI:10.1016/S0893-6080(09)80004-X.

González, A., Sala, A. and Armesto, L. (2022). Decentralized multi-agent formation control with pole-region placement via cone-complementarity linearization, *International Journal of Applied Mathematics and Computer Science* **32**(3): 415–428, DOI: 10.34768/amcs-2022-0030.

Hou, Z.S. (1994). *The Parameter Identification, Adaptive Control and Model Free Learning Adaptive Control for Nonlinear Systems*, Ph.D. thesis, Northeastern University, Shenyang.

Hou, Z. and Jin, S. (2010). A novel data-driven control approach for a class of discrete-time nonlinear systems, *IEEE Transactions on Control Systems Technology* **19**(6): 1549–1558.

Hou, Z.S. and Jin, S.T. (2013). *Model Free Adaptive Control: Theory and Applications*, CRC Press, Boca Raton, DOI: 10.1201/b15752.

Hou, Z.S. and Wang, Z. (2013). From model-based control to data-driven control: Survey, classification and perspective, *Information Sciences* **235**: 3–35.

Ignaciuk, P. (2015). Discrete-time control of production-inventory systems with deteriorating stock and unreliable supplies, *IEEE Transactions on Systems, Man and Cybernetics: Systems* **45**(2): 338–348, DOI: 10.1109/TSMC.2014.2347012.

Ivanov, D., Dolgui, A. and Sokolov, B. (2019a). The impact of digital technology and Industry 4.0 on the ripple effect and supply chain risk analytics, *International Journal of Production Research* **57**(3): 829–846, DOI: 10.1080/00207543.2018.1488086.

Ivanov, D., Dolgui, A. and Sokolov, B. (2019b). Ripple effect in the supply chain: Definitions, frameworks and future research perspectives, *in* D. Ivanov *et al.* (Eds), *Handbook of Ripple Effects in the Supply Chain*, Springer, Cham, pp. 1–33, DOI: 10.1007/978-3-030-14302-2_1.

Jarratt, T., Eckert, C.M., Caldwell, N.H. and Clarkson, P.J. (2011). Engineering change: An overview and perspective on the literature, *Research in Engineering Design* **22**(2): 103–124, DOI: 10.1007/s00163-010-0097-y.

Lee, H.L., So, K.C. and Tang, C.S. (2000). The value of information sharing in a two-level supply chain, *Management Science* **46**(5): 626–643, DOI: 10.1287/MNSC.46.5.626.12047.

Li, Q.K., Gao, X.F., Peng, C., Zhang, Y.L. and Yi, J. (2023). Data-driven change control design for product and supply chain synchronous evolution systems under cyber-attacks, *Scientia Sinica Informationis* **53**: 325–343, DOI: 10.1360/SSI-2021-0435, (in Chinese).

Li, Q.K., Lin, H., Tan, X. and Du, S. (2020). $H\infty$ consensus for multiagent-based supply chain systems under switching topology and uncertain demands, *IEEE Transactions on Systems, Man, and Cybernetics: Systems* **50**(12): 4905–4918, DOI: 10.1109/TSMC.2018.2884510.

Liang, J., Bu, X., Cui, L. and Hou, Z. (2021). Data-driven bipartite formation for a class of nonlinear MIMO multiagent systems, *IEEE Transactions on Neural Networks and Learning Systems* **34**(6): 3161–3173, DOI: 10.1109/TNNLS.2021.3111893.

Liu, Z., Jahanshahi, H., Volos, C., Bekiros, S., He, S., Alassafi, M.O. and Ahmad, A.M. (2021). Distributed consensus tracking control of chaotic multiagent supply chain network: A new fault-tolerant, finite-time, and chatter-free approach, *Entropy* **24**(1): 33, DOI: 10.3390/e24010033.

Luo, J., Yang, W., Ju, G. and Min, X. (2014). The study on consensus control of supply chain system based on multi-agent model, *Proceedings of the 2014 International Conference on Advanced Mechatronic Systems, Kumamoto, Japan,* pp. 526–531, DOI: 10.1109/ICAMechS.2014.6911602.

López-Estrada, F.-R., Darias, H., Puig, V., Valencia-Palomo, G., Domínguez-Zenteno, J. and Guerrero-Sánchez, M.-E. (2024). Cooperative convex control of multiagent systems applied to differential drive robots, *International Journal of Applied Mathematics and Computer Science* **34**(2): 199–210, DOI: 10.61822/amcs-2024-0014.

Notarnicola, I., Bin, M., Marconi, L. and Notarstefano, G. (2023). The gradient tracking is a distributed integral action, *IEEE Transactions on Automatic Control* **68**(12): 7911–7918, DOI: 10.1109/TAC.2023.3248487.

Patalas-Maliszewska, J., Posdzich, M. and Skrzypek, K. (2022). Modelling information for the burnishing process in a cyber-physical production system, *International Journal of Applied Mathematics and Computer Science* **32**(3): 345–354, DOI: 10.34768/amcs-2022-0025.

Patalas-Maliszewska, J., Wiśniewski, R., Zhou, M., Topczak, M. and Wojnakowski, M. (2024). Applying additive manufacturing technologies to a supply chain: A Petri net-based decision model, *International Journal of Applied Mathematics and Computer Science* **34**(3): 513–525, DOI: 10.61822/amcs-2024-0035.

Peng, C., Zhang, A. and Li, J. (2021). Neuro-adaptive cooperative control for high-order nonlinear multi-agent systems with uncertainties, *International Journal of Applied Mathematics and Computer Science* **31**(4): 635–645, DOI: 10.34768/amcs-2021-0044.

Rodrigues, L. and Boukas, E.K. (2006). Piecewise-linear $H\infty$ controller synthesis with applications to inventory control of switched production systems, *Automatica* **42**(8): 1245–1254, DOI: 10.1016/j.automatica.2006.04.004.

Sarimveis, H., Patrinos, P., Tarantilis, C.D. and Kiranoudis, C.T. (2008). Dynamic modeling and control of supply chain systems: A review, *Computers & Operations Research* **35**(11): 3530–3561.

Snyder, L.V. and Shen, Z.M. (2019). Applications of supply chain theory, *in* L.V. Snyder and Z.M. Shen (Eds), *Fundamentals of Supply Chain Theory*, John Wiley & Sons, Hoboken, pp. 615–642, DOI: 10.1002/9781119584445.ch16.

Ullah, I., Tang, D. and Yin, L. (2016). Engineering product and process design changes: A literature overview, *Procedia CIRP* **56**: 25–33, DOI: 10.1016/j.procir.2016.10.010.

Wang, Z., Wang, D., Lian, J., Ge, H. and Wang, W. (2024). Momentum-based distributed gradient tracking algorithms for distributed aggregative optimization over unbalanced directed graphs, *Automatica* **164**: 111596.

Wright, I. (1997). A review of research into engineering change management: Implications for product design, *Design Studies* **18**(1): 33–42, DOI: 10.1016/50142-694X(96)00029-4.

Xiong, S. and Hou, Z. (2021). Data-driven formation control for unknown mimo nonlinear discrete-time multi-agent systems with sensor fault, *IEEE Transactions on Neural Networks and Learning Systems* **33**(12): 7728–7742, DOI: 10.1109/TNNLS.2021.3087481.

Xu, L., Mak, S. and Brintrup, A. (2021). Will bots take over the supply chain? Revisiting agent-based supply chain automation, *International Journal of Production Economics* **241**: 108279, DOI: 10.1016/j.ijpe.2021.108279.

Zhao, K., Scheibe, K., Blackhurst, J. and Kumar, A.K. (2019). Supply chain network robustness against disruptions: Topological analysis, measurement, and optimization, *IEEE Transactions on Engineering Management* **66**(1): 127–139, DOI: 10.1109/TEM.2018.2808331.

Zhao, L. and Yu, J. (2017). Adaptive bipartite consensus tracking control for coopetition multi-agent systems with input saturation, *6th Data Driven Control and Learning Systems Conference, Chongqing, China*, pp. 383–386, DOI: 10.1109/DDCLS.2017.8068102.

Lingling Fan received her PhD degree from Beijing Jiaotong University, China, in 2017. She is currently an associate professor with the School of Automation, Beijing Information Science and Technology University. Her research interests cover multi-agent systems, pursuit-evasion, data driven control and supply chain systems.

Xiangchen Zeng received his BE degree from Beijing Information Science and Technology University in 2023. He is currently pursuing the MS degree with that University. His research interests cover multiagent systems, data-driven control and model-free adaptive control.

Shuangshuang Xiong received her master's degree in probability theory and statistics from Nanjing Normal University, China, in 2015, and her PhD degree in traffic information engineering and control from Beijing Jiaotong University, China, in 2020. She is an associate professor with the School of Automation, Beijing Information Science and Technology University. Her research interests cover data-driven control, model-free adaptive control and multiagent systems.

Qingkui Li received his BS degree in mathematics education from Shandong Normal University, Jinan, China, in 1998, his ME degree also in mathematics education from Liaoning Normal University, Dalian, China, in 2001, and his PhD degree in control theory and control engineering from Northeastern University, Shenyang, China, in 2009. From 2010 to 2012, he was a postdoctoral research fellow with the Centre for Intelligent and Networked Systems (CINS), Central Queensland University, Australia. He is currently a professor with the School of Automation, Beijing Information Science and Technology University, China. His present research interests include switched systems, networked control systems, and supply chain systems.

Received: 30 March 2025
Revised: 16 August 2025
Accepted: 7 September 2025